

Mapping of Soil-Geochemistry Using Pollution Migration Forecasts

Dr.D.K. Agrawal

Received: 19 June 2019 ▪ Revised: 17 July 2019 ▪ Accepted: 14 August 2019

Abstract: The transfer of hazardous synthetic substances into the groundwater environment is an extraordinary risk to general welfare and nature. Logical concerns are currently developing regarding predictive techniques that can be accessed for environmental assessment of fixed targets and synthetic spills. After considering various methods and geodata that could be included, the stagnant zone model was adopted. The main problems that need to be addressed here are budget resource regulation for surface fixation, risk assessment as well as acceptable synthetic substance enrichment. It is possible to generate numbers and to examine biology according to the proposed scientific model with organized parameters for the movement of pollutants and soil. The strategy considered can complement target exploration and support map geochemical mapping.

Keywords: Weather Conditions, Ecological Monitoring, Mapping Soil-geochemistry, Contamination Zone.

INTRODUCTION

Displacement of hydrogeological pollutants is based on observations based on perception of disturbance in invasion and drying of the soil under climatic conditions. The two-dimensional displacement model is the best method for calculating the fixation edge of the upper dirty water zone above the Vadose zone (Figure 1). The one-dimensional model, which represents the penetration and vertical development of water in a source, cannot be used here and there in the topsoil for long-term mass movement, because there is a constant pattern of development along with a tendency to be supported by pollution sources or watersheds (Celico, 2010). After obtaining various shift test compounds under local hydrogeological and climatic conditions, we can see a general part of the pressure-driven exchange process along the support angle along the slope (Khalil et al., 2013). Similarly, it is possible to make an appropriate numerical assessment of specific issues related to agriculture, agriculture, and organizational stages (Sadeghi et al., 2013). At the same time, we only limit the progress of geodatabase data to the CEO credit information interface to the initial and final state of the ground-water framework. This work shows a water-powered reconstruction model using a standing zone which is used when the mass is moved in a permeable environment (Lassin et al., 2005).

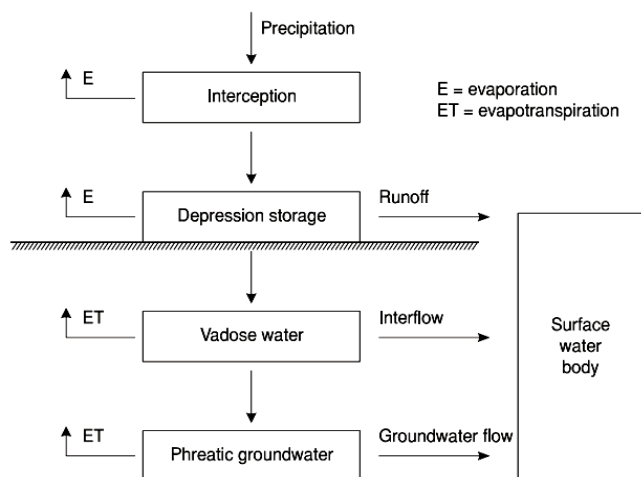


Figure 1: Elements of Hydrogeologic cycle

Despite the fact that there may be hypothetical explanations for the tendency of one model to another, decisions are regularly made for far wiser reasons. Drainage penetration also cannot be represented without limited conditions, just as the mass stroke parameters can be effectively characterized for a continuous process (Stinchcomb et al., 2016). It is difficult to choose conditions that limit the movement of pressure in groundwater with varying penetration speeds and soil moisture. In general, only a few parameters needed for a basic diagnostic strategy are available (Cascini, 2017). On the other hand, the detection of contaminant movements is limited to non-toxic (moderate) substances. Those who do not experience reaction or adsorption in dirty water. Improvements in the reactant recreation model are still ongoing.

For safeguarding soil and water resources, it is important to anticipate and assess the circulation of pollutant fixation in various parts of the contaminated area. Study information shows that drainage starts from the target over the contamination zone and reaches the compensation layer (Prunty and Casey, 2002; Tang et al., 2015). The most important problem that needs to be addressed here is the rate of development and focus on hazardous plastics. The recent advanced PC era offers a major office dashboard covering various sections of natural security related to biological assessments, land mapping, and geochemistry (Mosley et al., 2014). Around it, the spotlight is to offer a framework that is difficult to use by survey engineers from a controlled branch of ecological knowledge (Shah et al., 2014).

Based on soil surveys and plant geochemistry which has so far been carried out for the discussion area, the manner in which this movement strongly emphasizes the support and scope of the location in managing the main landscape is emphasized (Prunty & Casey, 2002).

BACKGROUND

The process of rinsing at the washing sites to a fixed target consists of three phases: drainage deposit, which is related to the time the water particles move to the control point, dynamic filtration to reduce the focus of pollutants and clean phase without contamination of the standing segment zone. It is clear that drainage at a good road checkpoint depends on the watershed and geodetic slope along the mass movement camp.

An important condition for mass movement between reaching individual water particles and standing areas can be evaluated by:

$$\frac{\partial(\varepsilon C)}{\partial t} = ks(C_1 - C) \quad (1)$$

$$\frac{\partial(\varepsilon_1 C_1)}{\partial t} = -ks(C_1 - C) \quad (2)$$

Where:

N - average concentration of contaminant in individual water particles, C - average concentration of contaminant in stagnate zones particles, ε - dimensionless specific volume of the water particles, ε_1 - dimensionless specific volume of the stagnate zones particles, t - time of contact between the water and stagnate zones particles, k, s - coefficient and specific surface of the mass-transfer.

According to the Lagrangian method, the following relationship is established to drive the axis and time system t associated with the single water particle provided conditions where, $e = \text{constant}$, $e_1 = \text{constant}$:

$$\varepsilon \frac{dC}{dt} = -\varepsilon_1 \frac{dC_1}{dt} \quad (3)$$

Using equation (2), this relation can be transformed by differentiating

$$\frac{d^3 C}{dt^3} = -Bks \frac{dC}{dt} \quad (4)$$

Where:

$$B = \frac{1}{\varepsilon_1} + \frac{1}{\varepsilon}$$

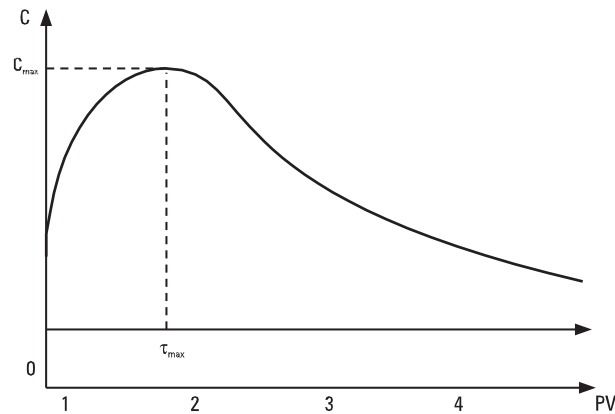


Fig. 2: Typical pollutant concentrations in water from lysimeter at the control limit with short rainfall t
(Source: authors' study)

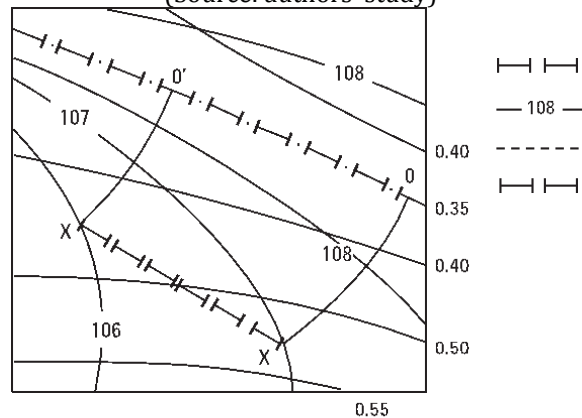


Fig.3: Contaminated site with relief and relational concentration isolines 00* – watershed, XX* – control border, - 108 -- relief gradient lines (Source: Author's study).

The first integral of equation (4) along a flow line of the water particles is:

$$\frac{dC}{dt} = C_0^* \exp(-Bkst) \quad (5)$$

Where:

$$C_0^* = \left(\frac{dC}{dt} \right)$$

- Initial rate of concentration change in water particles.

It is important to remember that C^* is only constant for each water particle that starts moving at the beginning of its individual time $t = 0$.

To find this constant, consider equation (2) written for solid particles from the standing zones which is at the starting point of water particles. Ax and system time are stationary and refer to the base-line stand area (water catchment area).

Then:

$$\varepsilon_1 \frac{dC_1}{d\tau} = -ks(C_1 - C) \quad (6)$$

$$\varepsilon_1 \frac{dC_1}{d\tau} = -\varepsilon \frac{\partial C}{\partial \tau} \quad (7)$$

Where:

t – time passed since start of the rain till the moment of contact with considering water particle, i.e. continuance of the rain (leaching).

Moreover, from equation (5) we can interpret:

$$C_0^* = \frac{ks}{\epsilon} (C_{10} - C_0) \exp\left(-\frac{ks\tau_0}{\epsilon_1}\right) \quad (8)$$

It should be noted that the decrease in the concentration of contamination at the control boundary can be explained by this expression when the first particle arrives at the control point from the starting point line (watershed). The actual pollutant concentration increases before this point $t < \int_0^{x_L} \frac{dx}{V_f}$ by the interrupted movement of the pollution concentration front with velocity v_f from watershed to the control border L (Figures 2 and 3).

It takes the form:

$$C = C_0 + \frac{1}{B\epsilon} (C_{10} - C_0) [1 - \exp(-Bkst)] \quad (9)$$

Thus, the embodiment of the proposed approach includes information on normal fixation for areas where surface contaminants might appear. At the same time, as part of a real environmental management sample, we must complete pollution and geochemical parameters for the total amount of soil and water structure under consideration (Grunsky et al., 2017).

METHODOLOGY

Assuming the active leaching process with decreasing of the pollutant concentration by native clean precipitation $C_0 = 0$, the equation (9) can be represented as:

$$-\ln \frac{C}{C_p} = -\ln \frac{1 - \exp(-BKT)}{B\epsilon} + \frac{K}{\epsilon_1} \tau \quad (10)$$

Where

$K = ks$ - volumetric coefficient of mass-transfer, $C_{10} = C_p$ - water solubility or other tabulated concentration, T - individual distance time of the mapping point, t - summary time of precipitation.

To elaborate on the beginning of the invasion and shift without subsequent effort, we set T as an important time for developing the front focus from the watershed to the mapping control point. In accordance with the application of strategies to evaluate the circulation of pollutants in the upper layers of dirty water, two perceptions can be made. In the isotropic underground, the results of the development of the isolated focus initially show a clear direction in the darkness of aid (Figures 4 and 5). Second, the volumetric mass transfer coefficient is determined as the deviation from the sloping side of the connecting line at each control point (Figure 6). However, we need two exploration focal points for two clear rainfall images to find the parameters

Tests must be completed for better ranking. In addition, there are three motor lines for the three control centers, which are located on the slope of the relief with equal separation from each other ($AB = BC$) and the geodetic equivalent of suffering from $HA - HB = HB - HC$ (Figure 4). In addition, it is important to have three test information (Figure 6) for reference controls that focus on lighting the country's economic development framework:

$$-\ln \frac{C_1}{C_p} = -\ln \frac{1 - \exp(-Bkt) \exp(-Bk\Delta t)}{B\epsilon} + \frac{k}{\epsilon_1} \tau \quad (11)$$

$$-\ln \frac{C_2}{C_p} = -\ln \frac{1 - \exp(-Bkt)}{B\epsilon} + \frac{k}{\epsilon_1} \tau \quad (12)$$

$$-\ln \frac{C_3}{C_p} = -\ln \frac{1 - \exp(-Bkt) \exp(Bk\Delta t)}{B\epsilon} + \frac{k}{\epsilon_1} \tau \quad (13)$$

where the physical state of the same slope is given by $DT \in T$. Obviously, the time distance for the upper point A is $T - DT$, for the center point B is T , for the lower point C is $T + DT$. Setting the specified parameters:

$$\frac{C_1}{C_p} \exp\left(\frac{K}{\varepsilon_1} \tau_1\right) = A_1$$

$$\frac{C_2}{C_p} \exp\left(\frac{K}{\varepsilon_1} \tau_1\right) = A_2 \quad (14)$$

$$\frac{C_3}{C_p} \exp\left(\frac{K}{\varepsilon_1} \tau_1\right) = A_3$$

After transforming the equations (14), we have:

$$(1 - B\varepsilon A_2)^2 = (1 - B\varepsilon A_1)(1 - B\varepsilon A_3) \quad (14)$$

Thus:

$$B\varepsilon = 1 + \frac{\varepsilon}{\varepsilon_1} = \frac{2A_2 - A_1 - A_3}{A_2^2 - A_1A_2} \quad (15)$$

Finally, the porosity parameter ε_1 , such as $m = \varepsilon_1 + \varepsilon$, individual K values for each soil are obtained with experimental data and equation (4). The time intervals T and DT can be determined by equation (14) for the image control points.

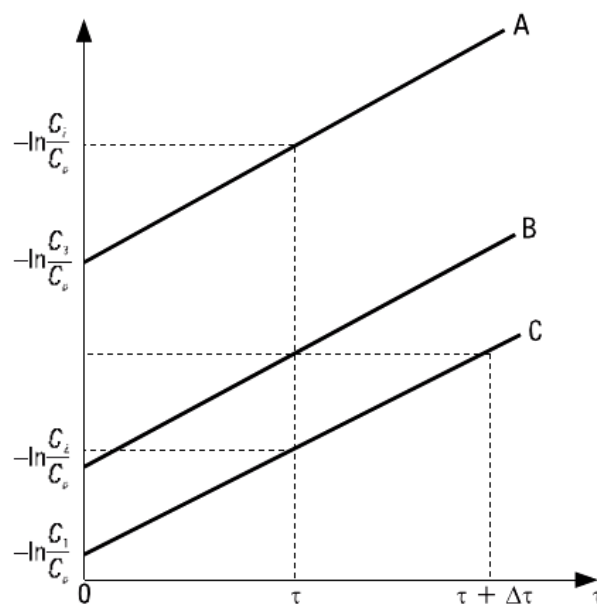


Fig.4: Kinetic lines for the control points ABC (Source: Author)

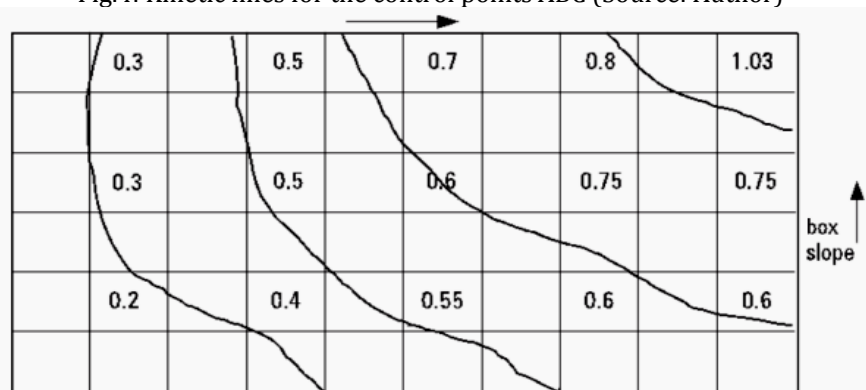


Fig.5: The related conductivity of the initial equivalent sand after the equivalent precipitation

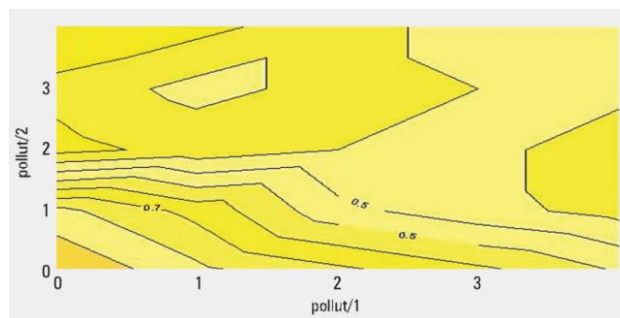


Fig.6: Surface soil-geochemistry mapping for contaminated site at 3PV precipitation

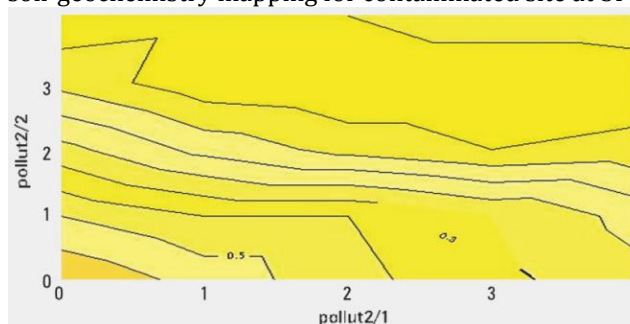


Fig.7: Surface soil-geochemistry mapping for contaminated site at 5 PV precipitation (forecast for relational concentration of contaminant in lysimeter outlet water)

RISK ASSESSMENT

Assessing and shaping the results of traffic to a site is very difficult to prepare because the idea of delay can be changed in this way. There are also differences in movement between pollutants in different groundwater frames. At this point, a toxicological risk assessment of the cause of protection for any impurities must be submitted. Under certain conditions, limiting pollutants can enter ground water and surface water.

Most likely intrusion into the buoy and overflows from the site under discussion. Therefore, some experts issue an order stipulating that limiting pollutants in the most extreme focus does not have access to limiting pollutants in lysimeter springs. On the other hand, the current explanation method is now ready to distinguish other sizes of synthetic substances in water, which are available here and there in focus and far below which can have harmful effects.

Before using landfills or plastics, extensive study of their natural behavior must be carried out. At the same time, computer projects and sophisticated verification tools violate the mapping and data control processes. With real natural administration, it is possible to assess hazards in terms of the number of accidents detected to limit pollutants to the control limits.

DISCUSSIONS

To distinguish between these properties from intrusive movement systems, we must find the dependence of their connection test of sufficient performance (snow softening). The similarity of test curves associated with obstacles such as continuous systems creates goals behind old points of the proposed model under local climate conditions (see Figure 3).

Two-dimensional studies were carried out on thin-film models. Examples of impurities are put in a $100 \times 60 \times 10$ cm box. To measure the spread of fixation in a single layer, it is first important to apply a condrometer strategy. The results of social conductivity show that the redistribution of pollution caused by rain is highly dependent on housing trends, floor structure and good individual understanding (Figure 7).

The main use of this study is the prediction of contamination zones as a biological result of the displacement of components in soil and water. The effects of the actual scene display (Figure 3) and climate conditions are introduced as the accumulation of social pollution (Figures 7 and 8) for normal focus areas. The geochemical mapping of this soil shows remarkable changes in the isolated binding due to the relief, the geotechnical nature of the soil and the strength of precipitation.

CONCLUSION

The consequences of environmental damage from landfills, silos, spills or undeveloped rural practices can be prevented by successful geotechnical structural methods, environmental verification and safe use of agrochemicals.

To limit the development of synthetic compounds in ground water and surface water, it may be important to take measurements of the length of nature (a count of the geochemical mapping of the soil) given the PC's reproduction of disturbances with mass movements in the ground water frame.

The natural movement of hazardous synthetic mixes depends on aid, climate, hydrogeological conditions, pH values as well as redox conditions and propagation properties.

The proposed technique should, as far as possible, be given information about testing active ingredients for different soils under local conditions for long excavations.

REFERENCES

- [1] Celico F., Naclerio G., Bucci A., Nerone V., Capuano P., Carcione M., Allocca V. & Celico P., Influence of pyroclastic soil on epikarst formation: A test study in southern Italy. *Terra Nova*, (2010), 22: 110–115.
- [2] L.Cascini, M. Ciurleo, and S. Di Nocera, "Soil depth reconstruction for the assessment of the susceptibility to shallow landslides in fine-grained slopes," *Landslides*, vol. 14, no. 2, pp. 459–471, 2017.
- [3] Lassin et al., 2005 A. Lassin, M. Azaroual and L. Mercury, Geochemistry of unsaturated soil systems: aqueous speciation and solubility of minerals and gases in capillary solutions, *Geochim. Cosmochim. Acta* 69 (2005), pp. 5187–5201.
- [4] Prunty and Casey, 2002 L. Prunty and F.X.M. Casey, Soil water retention curve description using a flexible smooth function, *Vadose Zone J.* 1 (2002), pp. 179–185.
- [5] Sadeghi M, Morris GA, Carranza EJ, Ladenberger A, Andersson M. Rare earth element distribution and mineralization in Sweden: an application of principal component analysis to FOREGS soil geochemistry. *Journal of geochemical exploration*. 2013 Oct 1; 133: 160-75.
- [6] Shah, J., Jefferson, I. and Hunt, D.V.L. Resilience Assessment for Geotechnical Infrastructure Assets. *Proc. Institute of Civil Engineers: Asset Management* (2014).
- [7] Tang, J. & Riley, W. J. Weaker soil carbon-climate feedbacks resulting from microbial and abiotic interactions. *Nature Clim. Change* (2015), 5, 56–60.
- [8] Song L, Jian J, Tan DJ, Xie HB, Luo ZF, Gao B. Estimate of heavy metals in soil and streams using combined geochemistry and field spectroscopy in Wan-sheng mining area, Chongqing, China. *International Journal of Applied Earth Observation and Geoinformation*. (2015), 34, 1-9.
- [9] Stinchcomb GE, Nordt LC, Driese SG, Lukens WE, Williamson FC, Tubbs JD. A data-driven spline model designed to predict paleoclimate using paleosol geochemistry. *American Journal of Science*. 2016 Oct 1; 316(8):746-77.
- [10] Khalil A, Hanich L, Bannari A, Zouhri L, Pourret O, Hakkou R. Assessment of soil contamination around an abandoned mine in a semi-arid environment using geochemistry and geostatistics: pre-work of geochemical process modeling with numerical models. *Journal of Geochemical Exploration*. 2013 Feb 1; 125: 117-29.
- [11] Mosley, Luke M., Rob W. Fitzpatrick, David Palmer, Emily Leyden, and Paul Shand. "Changes in acidity and metal geochemistry in soils, groundwater, drain and river water in the Lower Murray River after a severe drought." *Science of the Total Environment* 485 (2014): 281-291.
- [12] Grunsky EC, de Caritat P, Mueller UA. Using surface regolith geochemistry to map the major crustal blocks of the Australian continent. *Gondwana Research*. 2017 Jun 1; 46: 227-39.